ELSEVIER

Journal of Photochemistry and Photobiology A: Chemistry 108 (1997) 179–185

Journal of PHOTOCHEMISTRY AND PHOTOBIOLOGY A: CHEMISTRY

Photoconductive and photocatalytic properties of $ZrTiO_4$. Comparison with the parent oxides TiO_2 and ZrO_2

J.A. Navio [a,*], G. Colón [a], J.M. Herrmann [b]

[a] *Instituto de Ciencia de Materiales de Sevilla, Centro Mixto CSIC-Universidad de Sevilla and Departamento de Química Inorgánica, Facultad de Química, E-41012 Sevilla, Spain*

[b] *URA au CNRS "Photocatalyse, Catalyse et Environnement", Ecole Centrale de Lyon, BP 163, 69131 Ecully Cedex, France*

Received 11 November 1996; accepted 6 February 1997

Abstract

Orthorhombic $ZrTiO_4$ was synthesized at 700 °C with a large surface area (39.5 $m^2\ g^{-1}$) and an appropriate band gap energy (3.33 eV) for the absorption of near-UV photons. Photoconductivity measurements were performed in vacuum and in oxygen to correlate the photoelectronic properties of $ZrTiO_4$ with its photocatalytic activity. $ZrTiO_4$ becomes a photoconductor on exposure to near-UV illumination due to electron–hole pair formation. On continuous evacuation, a very limited quantity of chemisorbed oxygen is photodesorbed because $ZrTiO_4$ is an insulator in the dark (no accumulation of extra photoelectrons corresponding to the consumption of holes for oxygen desorption). Photoconductivity isotherms ($\sigma = f(P_{O2})$) indicate that oxygen chemisorbs as non-dissociated O_2^- species, confirming previous results of oxygen isotopic exchange. $ZrTiO_4$ is photoactive for isopropanol oxidation, but much less active than titania and zirconia (the parent oxides), although it has a comparable surface area and UV light absorbance. The smaller photocatalytic activity is related to the more limited capacity to photoadsorb and photodesorb oxygen and a higher electron–hole recombination. This study confirms that binary oxides are less active than pure oxides and that titania (anatase) is the most active photocatalyst. © 1997 Elsevier Science S.A.

Keywords: Photocatalysis; Photoconductivity; TiO_2; ZrO_2; $ZrTiO_4$

1. Introduction

Certain solids, mainly chalcogenides (oxides, sulphides, etc.), act as photoconductors on illumination with near-UV photons. If the two photoinduced charge carriers, electrons and holes, do not recombine, they can reach the surface and react with chemisorbed species (electrons reacting with acceptors giving reduction reactions and holes reacting with donors giving oxidation reactions) [1]. The first reactions of this type investigated concerned mainly mild oxidation reactions of organic or inorganic compounds. More recently, oxidations have been performed in aqueous media, and total oxidation with the production of CO_2 and H_2O has been observed for organic compounds [2–4]. Of the various pure oxides, titania has been found to be the best photocatalyst, especially in its anatase form.

In this study, zirconium titanate ($ZrTiO_4$) is proposed as a potential photocatalyst. Care has been taken to synthesize $ZrTiO_4$ with a fairly large surface area [5], of the order of approximately 50 $m^2\ g^{-1}$, in order to obtain textural properties similar to that of titania Degussa P-25, which is generally chosen worldwide as a reference catalyst [1–4]. Mixtures of phases or impure (doped) phases produce inhibiting effects in photocatalysis [6–8]. In the present case, a pure phase $ZrTiO_4$ sample was used, which had been prepared according to Ref. [5] at a fairly low temperature (640 °C), compatible with both textural and structural requirements.

To determine the inherent photocatalytic activity of $ZrTiO_4$ and to compare it with those of the parent oxides, zirconia and titania, a well-known reaction was chosen, namely isopropanol photo-oxidation to acetone. The reaction mechanism has been studied previously by Bickley et al. [9,10] and Cundall et al. [11,12]. The same reaction has been chosen as a test reaction to establish the photocatalytic activity and photocatalytic inertness of pigments based mainly on TiO_2 and ZnO [13,14].

In a preliminary study, it has been shown that $ZrTiO_4$ is photosensitive in the near-UV region and can give, to some extent, oxygen isotopic exchange (OIE) following a type III mechanism, i.e. involving non-dissociated oxygen molecules chemisorbed and photoexcited at the surface [15]. It has also been shown that $ZrTiO_4$ becomes a photoconductor on illu-

* Corresponding author. Tel.: +34 5 4557161; fax: +34 5 4557134.

PII S1010-6030(97)00080-4

mination [15] and is photocatalytically active [16]. The aim of this study was to correlate the photocatalytic activity and photoelectronic properties of $ZrTiO_4$ in order to account for its photoactivity and for the differences observed with the two parent oxides ZrO_2 and TiO_2. Photoconductance measurements were used to follow the photoelectronic response of the different catalysts as a function of various parameters, such as the light intensity, vacuum and oxygen partial pressure [17].

2. Experimental details

2.1. Photoconductivity cell

The previously described photoconductivity cell [17] was connected to a grease-free and mercury-free vacuum system (residual pressure, approximately 10^{-6} Torr). It contained a frame with two parallel gold electrodes which were found to be photoinactive under oxygen. The powder sample was lightly compressed to form a pellet in the frame which was disposed perpendicularly to the radiant flux. UV light was provided by a Philips HPK 125 W mercury lamp, whose output was filtered by a water-circulating cuvette and Pyrex optical windows, so that $ZrTiO_4$ was maintained at room temperature and received photons of energy higher than the band gap (3.33 eV).

2.2. Photoreactor

The photoreactor used for carrying out isopropanol photooxidation was an Applied Photophysics Ltd. photochemical reactor equipped with a 400 W medium pressure mercury arc lamp, radiating predominantly at 365–366 nm. This lamp produced more than 5×10^{19} photons s^{-1} within the reaction flask. It was contained in a doubled-glass immersion well, through which water was passed for cooling. A borosilicate glass sleeve was used to remove short-wavelength radiation (less than 300 nm). A gas inlet reaction flask (400 ml) was used; a double surface condenser was fitted to the reaction flask to prevent ;''creep'' and loss of vapour. The reaction was performed at room temperature (approximately 300 K).

2.3. Materials

Powdered zirconium titanate was processed following the sol–gel method described previously [5]. The amorphous solid was precipitated by hydrolysis in an alcoholic solution containing equimolar amounts of $TiCl_4$ (Merck, 99.99%) and $ZrOCl_2$ (Fluka AG, 43%–44%, ZrO_2) in the presence of an excess of hydrogen peroxide. The precipitate was washed, dried and calcined at 700 °C for 2 h; the solid obtained had the structure of crystalline $ZrTiO_4$ in the orthorhombic form. A zirconia gel powder was also prepared via the hydrolysis of $ZrOCl_2$ using an aqueous solution of ammonium hydroxide at pH 11. After washing and drying, this amorphous zirconia powder was calcined at 1000 °C for 2 h; the solid obtained had the structure of crystalline ZrO_2 in the monoclinic phase and is referred to hereafter as ZrO_2 (hp). Commercial titanium dioxide TiO_2 and zirconium dioxide ZrO_2 were supplied by Degussa, and before use were calcined in air at 500 °C for 2 h. X-Ray diffraction showed that ZrO_2 (Degussa) was a mixture of the monoclinic and (mainly) tetragonal phases. The thermal treatments of the above samples were chosen on the basis of previously reported characterizations [5,18,19]. Isopropanol and other reagents were of analytical grade.

2.4. Photoconductivity measurements

For the photoconductivity measurements, the sample was first dried at 110 °C for 45 min to obtain better pelletization. Once settled in the frame, the sample was evacuated for 15 h under a dynamic vacuum (residual pressure, less than 10^{-6} Torr). Since the exact depth of penetration of the UV beam into the pelletized sample is not known, the geometric factor of the photoconductivity σ ($ohm^{-1}\,cm^{-1}$) cannot be determined. σ was assumed to represent the photoconductance ($\sigma = 1/R$ in ohm^{-1}, where R is the photoresistance measured).

For the photocatalytic runs, the photocatalysts (1.5 g of each) were independently suspended in pure dried isopropanol (300 ml). Air or pure oxygen was bubbled through the suspension and a positive pressure of the gas was maintained during the period of illumination (6 h). The photocatalyst was separated by centrifugation to analyse the liquid phase. Samples from the photoreaction mixture were analysed by a Hewlett-Packard gas chromatograph (model 5890) equipped with a 2.1 m column of 10% polyethylene glycol on Chromosorb W at 343 K, which gave a good separation of diethyl ether, acetone and isopropanol. N_2 was used as carrier gas (1.6 ml s^{-1}).

3. Results and discussion

3.1. Electrical photoconductivity of $ZrTiO_4$

3.1.1. Under vacuum

The electrical conductivity of $ZrTiO_4$ in the dark under dynamic vacuum ($P<10^{-5}$ Torr) is less than 1×10^{-14} ohm^{-1}, this being the lower limit of detection of the instrument. On UV illumination, there is an instantaneous increase in the photoconductance σ, reaching a value of 2×10^{-12} ohm^{-1} within 30 s (Fig. 1). The photoconductance continues to increase for 4 h before reaching a plateau at $\sigma\approx10^{-11}$ ohm^{-1}, which corresponds to a steady state between the generation rate G of the photoinduced electrons and holes and their recombination rate R. When UV illumination is suppressed, the conductance decreases to 10^{-14} ohm^{-1}. Further illumination with the same radiant flux allows the solid to recover instantaneously to the photoconductance level obtained at the end of the first UV period. This phenomenon

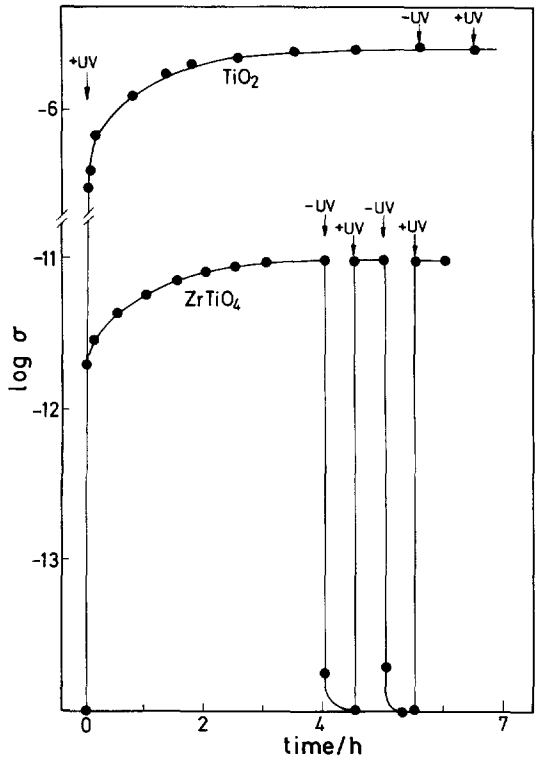

Fig. 1. Kinetics ($\log \sigma = f(t)$) of the photoconductance σ (ohm^{-1}) of $ZrTiO_4$ under dynamic vacuum (less than 10^{-6} Torr) during the first UV illumination ($t=0$) and after subsequent periods in the dark and further exposure to UV illumination. Comparison with titania Degussa P-25.

is reproducible (Fig. 1). This behaviour can be explained by comparison with TiO_2 under identical conditions (Fig. 1). The photoconductance of TiO_2 gives larger variations until reaching the steady state. This requires a longer time (approximately 7 h), but yields a photoconductance level of about 10^{-7} ohm^{-1}, i.e. four orders of magnitude higher. This increase in σ has been ascribed to the creation of electron–hole pairs in the semiconductor (SC)

$$SC + h\nu \rightarrow e^- + p^+ \quad (h\nu \geq E_G) \tag{1}$$

followed by the photodesorption of ionized oxygen species which cannot be desorbed under vacuum in the dark [17]

$$O_x^- + p^+ \rightarrow \frac{x}{2}O_2(g) \quad \text{with } x = 1 \text{ or } 2 \tag{2}$$

This photodesorption is detected by an increase in pressure in the cell on exposure to UV irradiation. From Eqs. (1) and (2), an excess of photoelectrons over photoproduced holes occurs, since the latter are created in a quantity equal to that of the electrons, but are partially consumed by Eq. (2) before reaching the steady state governed by the equality $G = R$. The total concentration $[e]_T$ of electrons present on UV illumination is equal to

$$[e]_T = [e]_0 + [e]_t \tag{3}$$

where $[e]_0$ is the concentration of electrons accumulated during the photodesorption of the oxygen species (Eq. (2)) and $[e]_t$ is the instantaneous concentration of photogenerated electrons. In the case of TiO_2, the conductance does not change when the illumination is stopped [17]. This means that, in Eq. (3), $[e]_0 \gg [e]_t$.

By contrast, for $ZrTiO_4$, a decrease in σ is observed in the dark (Fig. 1). This indicates that, in Eq. (3), the instantaneous concentration of electrons photogenerated at time t is important with respect to $[e]_0$. As soon as the dark condition is re-established, the electrons recombine with the previously photogenerated holes. Consequently, the photoconductivity σ drops to a very low level proportional to $[e]_0$. This means that, under the radiant flux used, the photodesorption of oxygen on $ZrTiO_4$ is limited and is much smaller than that for TiO_2.

This behaviour is similar to that observed for CdS [20] for which a very low amount of photodesorbed species is detected.

3.1.2. Under an oxygen atmosphere

The photoconductance variations as a function of the oxygen pressure enable the nature of the ionosorbed oxygen species to be determined on exposure to UV light. The oxygen pressure was varied over three orders of magnitude (from 5×10^{-3} to 5 Torr). The first dose of oxygen caused an initial small decrease in σ, ascribed to a limited photoionosorption of oxygen, followed by a limited increase in σ associated with a possible subsequent photodesorption of oxygen species. The phenomena are very limited and, according to a log–log plot of the isotherm $\sigma = f(P_{O2})$ (Fig. 2), it can be established that, below 10^{-1} Torr, the oxygen pressure has practically no influence on σ. However, for 10^{-1} Torr $\leq P_{O2} \leq 5$ Torr, σ varies inversely with P_{O2} according to the slope $d \log \sigma / d \log P_{O2}$ equal to -1

$$\sigma = kP_{O2}^{-1} \tag{4}$$

The solid is in equilibrium with gaseous oxygen on exposure to UV light, but, when UV illumination is stopped, the conductance falls rapidly to 1×10^{-14} ohm^{-1}, confirming the trapping of electrons by ionosorbed oxygen. Further UV illumination under a constant radiant flux enables the solid to recover its previous photoconductance.

For decreasing oxygen pressures, the electrical photoconductivity σ measured at steady state varies first as $P_{O2}^{-0.8}$ for $P_{O2} > 10^{-1}$ Torr (Fig. 2(B)) and subsequently becomes independent of P_{O2}. These results can be interpreted within the framework of an oxygen ionosorption model previously proposed for various semiconductor oxides [17]

$$O_2(g) \rightarrow O_2(ads) \tag{5}$$

$$O_2(g) \rightarrow 2O(ads) \tag{6}$$

$$O_2(ads) + e^- \rightarrow O_2^-(ads) \tag{7}$$

$$O(ads) + e^- \rightarrow O^-(ads) \tag{8}$$

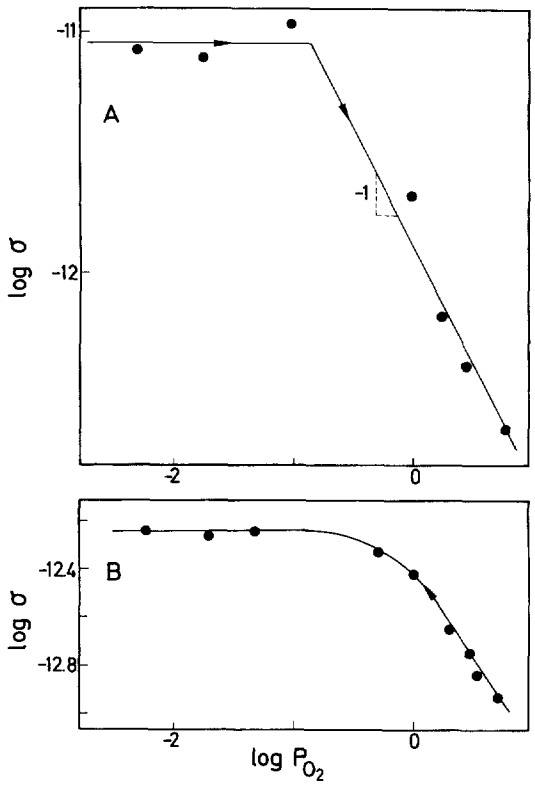

Fig. 2. Isotherms $\log \sigma = f(\log P_{O2})$ of the photoconductance σ (ohm^{-1}) measured at the steady state (see Fig. 1): curve A, increasing oxygen pressure from 10^{-3} to 5 Torr; curve B, decreasing oxygen pressure.

The formation of O_2^- and O^- ionosorbed species enables the general expression of the photoconductance σ measured at steady state to be determined [17]

$$\sigma = \frac{AG}{k_7 K_5 P_{O2} + k_8 K_6 P_{O2}^{1/2} + k_r[p^+]} \quad (9)$$

where A is a coefficient which includes the electron charge and mobility as well as the textural parameters of the semiconductor considered, G is the generation rate of photoproduced electrons and holes (Eq. (1)), k_i and K_i are the usual rate and equilibrium constants relative to Eq. (i) and k_r is the rate constant of recombination of the electrons and holes. Eq. (9) implies that the contribution of the non-illuminated part of the pellet to the resistance measured is negligible, which is true for $ZrTiO_4$ as for TiO_2 [17] and CdS [20]. In the low oxygen pressure region in which $d\sigma/dP_{O2} = 0$, the two terms including P_{O2} in the denominator are negligible with regard to $k_r[p^+]$. Since $\sigma = A[e^-]$, Eq. (9) becomes equivalent to $G = k_r[p^+][e^-]$, i.e. most of the photocreated electrons and holes recombine. When P_{O2} is increased, the terms including P_{O2} increase and, for $P_{O2} > 10^{-1}$ Torr, the term $k_7 K_5 P_{O2}$ becomes important, and Eq. (9) becomes equal to

$$\sigma = \frac{AG}{k_7 K_5 P_{O2}} \propto P_{O2}^{-1} \quad (10)$$

This means that, in the pressure range investigated ($10^{-1} \leq P_{O2} \leq 5$ Torr), oxygen photoadsorbs principally in the form of non-dissociative O_2^- species.

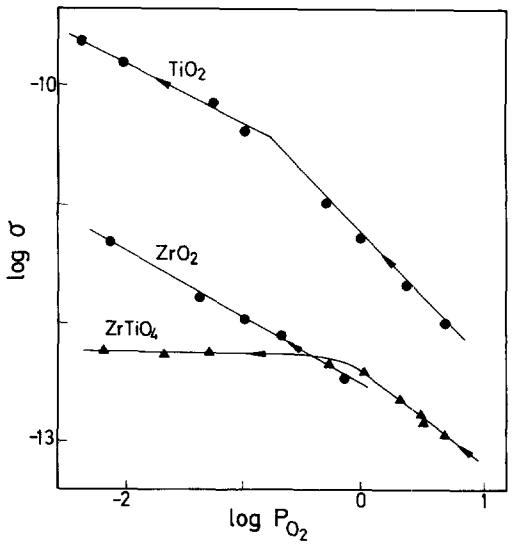

Fig. 3. Comparison of the isotherms $\log \sigma = f(\log P_{O2})$ of TiO_2, ZrO_2 and $ZrTiO_4$ determined at decreasing oxygen pressure.

When the oxygen pressure is decreased stepwise (Fig. 2(B)), σ varies first as P_{O2} and, below 10^{-1} Torr, becomes independent of P_{O2}. The value of the exponent is still close to -1, but corresponds to an apparent order. This means that the O_2^- adsorbed species which are in equilibrium with ambient oxygen are progressively photodesorbed. The apparent order of 0.8 can be mathematically accounted for by the relative influence of each of the three terms in the denominator of Eq. (9). It can be asserted that, for $0.1 < P_{O2} < 5$ Torr, the main contribution to the expression of σ in Eq. (9) is given by $k_7 K_5 P_{O2}$, whereas below $P_{O2} = 10^{-1}$ Torr, the last term relating to recombination exclusively accounts for σ variations.

Because of the two extreme behaviours of σ ($\sigma = kP_{O2}^0$ or $\sigma = k' P_{O2}^{-1}$), it does not seem probable that the intermediate term $k_8 K_6 P_{O2}^{1/2}$ should intervene in Eq. (9). This means that O^- photoadsorbed species do not exist on $ZrTiO_4$. This may be due to the absence of dissociative adsorption sites, illustrated by Eq. (6), on this solid. This behaviour has never been observed previously for the various oxides studied [17]. It seems inherent to $ZrTiO_4$, because both titanium and zirconium dioxide, the parent oxides of zirconium titanate, can photoadsorb oxygen as O^- species [17], as confirmed by the $\log \sigma = f(\log P_{O2})$ isotherms of Fig. 3. Such results suggest that the photocatalytic process involved in the test reaction is different from that encountered for TiO_2 and ZrO_2.

3.2. Photocatalytic activity

The kinetics of photocatalytic oxidation of neat liquid isopropanol in contact with $ZrTiO_4$ are presented in Fig. 4. For comparison with the two parent oxides, this reaction was performed with titania (Degussa P-25) and two pure zirconia samples (Degussa and a home-prepared sample). The reaction was performed using ambient air as the oxidizing agent. It has been shown previously that the photocatalytic oxidation

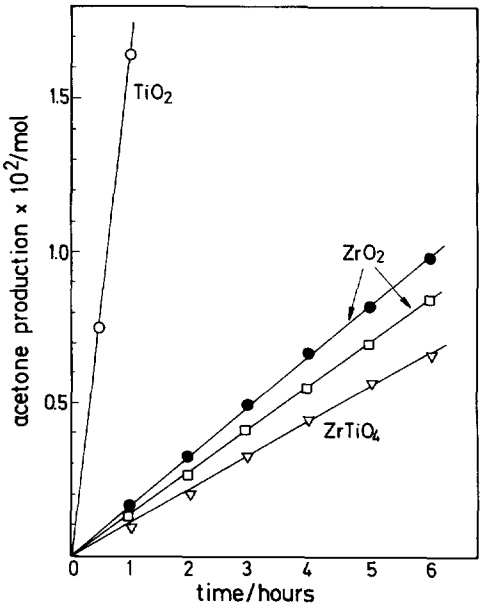

Fig. 4. Kinetics of acetone formation in the mild photocatalytic oxidation of isopropanol: ●, ZrO_2 (Degussa); □, home-prepared zirconia.

requires the simultaneous presence of UV radiation and gaseous oxygen [16]. The only organic product detectable by gas chromatography (GC) in the liquid phase was acetone. Therefore the overall photocatalytic reaction rate was chosen as the rate of acetone production. It follows a zeroth kinetic order with respect to time for all the catalysts under study, which can be explained by a maximum surface coverage θ in isopropanol

$$r = k\theta = kKC/(1+KC) \approx k \quad (\text{with } KC \gg 1)$$

The identical kinetic order enables the activities of the different samples to be compared. For a better comparison, the photocatalytic activities were expressed as the initial overall rates, and the corresponding specific rates (rates per unit of mass of catalyst in mmol h^{-1} (g catalyst)$^{-1}$) and intrinsic (or areal) rates (rates per unit of surface area in mmol h^{-1} m^{-2}). The different values are listed in Table 1. The following activity order was found, irrespective of the type of activity considered (Table 1): $TiO_2 \gg ZrO_2 > ZrTiO_4$.

It is confirmed that titania, especially the anatase form, is the most active solid. Zirconia is substantially less active than titania, but can still be considered as a potential photocatalyst for mild oxidation reactions [17,21]. The least active solid is $ZrTiO_4$.

The two ZrO_2 samples have comparable photoactivities, although their diffuse reflectance spectra, described in Ref. [16], have contrasting forms, ZrO_2 Degussa absorbing at much shorter wavelengths. It can be proposed that, for a given light flux, the smaller amount of photons absorbed by ZrO_2 Degussa can generate more efficient electron–hole pairs, which preferentially separate instead of recombining. Secondly, ZrO_2 Degussa possesses good adsorptive properties with respect to the reactants, thus favouring reactions in the adsorbed phase and compensating for its lower absorbance in the UV range used.

3.3. Correlations between the photoconductive and photocatalytic properties

The photocatalytic activity pattern $TiO_2 \gg ZrO_2 > ZrTiO_4$ clearly indicates a "negative synergistic effect", which produces an important decrease in activity for the solid resulting from the combination of two photoactive oxides. $ZrTiO_4$ is a well-defined solid [5], whose specific area (39.5 m^2 g^{-1}) and band gap energy (3.33 eV) [16] are close to those of titania and zirconia and cannot constitute textural and structural inhibiting factors.

The large discrepancy in activity between TiO_2 and $ZrTiO_4$ can be correlated initially with the large discrepancy observed in their electrical photoconductivities under vacuum (Fig. 1). Under identical UV illumination, titania can create more electron–hole pairs (Eq. (1)) and, consequently, more photoholes can desorb more ionosorbed oxygen species (Eq. (2)). However, $ZrTiO_4$ has an absorption spectrum close to that of zirconia and titania. Therefore it seems more probable that the better photocatalytic activity of titania is related to a more efficient separation of the electron–hole pairs or to a substantially lower tendency of recombination of electrons and holes. The curves of Fig. 1 clearly illustrate a higher photoinduced electronic activity for titania.

The discrepancy in activity between TiO_2 and $ZrTiO_4$ can also be accounted for by the photoconductivities in oxygen. The efficiency of $ZrTiO_4$ for the ionosorption of oxygen (Eqs. (5) and (7)) is much less than that of TiO_2. As soon as the first pulse of oxygen is introduced in contact with TiO_2 previously treated under dynamic vacuum and UV light, the photoconductivity decreases strongly by several orders of magnitude. For $ZrTiO_4$, the oxygen pressure must exceed 10^{-1} Torr to induce a decrease in σ.

Table 1
Photocatalytic activities of $ZrTiO_4$, ZrO_2 and TiO_2 in the oxidation of liquid isopropanol

Photocatalyst	Surface area (m^2 g^{-1})	Initial reaction rate (mmol h^{-1})	Initial specific rate (mmol h^{-1} (g catalyst)$^{-1}$)	Initial intrinsic (areal) rate (mmol h^{-1} m^{-2})
$ZrTiO_4$	39.5	1.17	0.78	2.0×10^{-2}
TiO_2 (Degussa)	46.5	15.0	10.0	0.215
ZrO_2 (Degussa)	35.4	1.63	1.09	3.08×10^{-2}
ZrO_2 (home-prepared)	23.4	1.41	0.94	4.02×10^{-2}

Table 2
Ionosorbed oxygen species and corresponding oxygen isotopic exchange (OIE)

Photocatalyst	d log σ/d log P_{O2}	Oxygen species ionosorbed	OIE mechanism	Reference
TiO_2	−1	O_2^-	II	[22]
	−1/2	O^-		
ZrO_2	−1/2	O^-	II	[23]
$ZrTiO_4$	−1	O_2^-	III	[15]

In addition, the isotherm log $\sigma = f(\log P_{O2})$ of Fig. 2 indicates the presence of only O_2^- species at the steady state, whereas titania adsorbs both O^- and O_2^- species and zirconia adsorbs only O^- species. The existence of dissociated O^- on TiO_2 and ZrO_2 has been confirmed by the nature of the mechanism of OIE [22,23]. The existence of O_2^- on $ZrTiO_4$ has also been confirmed by OIE [15]. In the presence of adsorbed O^-, OIE gives the so-called mechanism II induced by reaction (11)

$$^{16}O^-(ads) + {}^{18}O_2(g) \rightarrow {}^{16}O{}^{18}O(g) + {}^{18}O^-(ads) \quad (11)$$

In the presence of O_2^-(ads), the reaction of OIE follows the mechanism corresponding to the reaction

$$^{16}O_2^-(ads) + {}^{18}O_2(g) \rightarrow {}^{18}O_2^-(ads) + {}^{16}O_2(g) \quad (12)$$

This is summarized in Table 2. It has been shown that OIE and mild oxidation of alkanes on illuminated titania are competitive reactions and that OIE is initiated only when the alkane reaction is complete [23]. This clearly demonstrates that both reactions compete for the same photoactivated oxygen species, which is, according to mechanism II, a dissociated oxygen species

$$O^-(ads) + p^+ \rightarrow O^*(ads) \quad (13)$$

Such an active species can either give OIE according to Eq. (11) or alkane oxidation by insertion into a C–H bond [24], giving a "hot" molecule of alcohol, similar to observations in the gas phase [25]

$$R\text{–}CH_3 + O^* \rightarrow R\text{–}CH_2OH \quad (14)$$

Such an active species was estimated to be responsible for the mild oxidation reactions observed in pure organic media in the absence of water [21]. By contrast, in the presence of water, photoholes react preferentially with surface hydroxyl groups OH^-, which give, after successive hydroxylation reactions, total degradation products [1–4]. In the present case, the existence of O_2^- species detected on $ZrTiO_4$ by electrical photoconductivity is in agreement with the mechanism of isopropanol oxidation proposed by Bickley et al. [9,10] involving the following steps:

1. the separation of electrons and holes by reaction with O_2 and OH^- respectively

$$OH_s^- + p^+ \rightarrow OH_s^{\bullet} \quad (15)$$

$$O_2 + e^- \rightarrow O_2^-(ads) \quad (16)$$

2. H-atom abstraction by $OH^{\bullet}$ radicals

$$OH_s^{\bullet} + Me_2CHOH \rightarrow H_2O + Me_2C^{\bullet}OH \quad (17)$$

3. reactions of O_2^- with protons from water

$$O_2^- + H_2O \rightarrow HO_2^{\bullet} + OH_s^- \quad (18)$$

4. acetone formation from various reactions involving $Me_2C^{\bullet}OH$ radicals

$$Me_2C^{\bullet}OH + HO_2^{\bullet} \rightarrow Me_2CO + H_2O_2 \quad (19)$$

$$Me_2C^{\bullet}OH + O_2 \rightarrow Me_2CO + HO_2^{\bullet} \quad (20)$$

$$2Me_2C^{\bullet}OH \rightarrow$$

$$Me_2CO + Me_2CHOH \text{ (disproportionation)} \quad (21)$$

This mechanism accounts for isopropanol oxidation on $ZrTiO_4$ and can also account for that performed on titania. However, on titania, the formation of dissociated oxygen species O*(ads) may also be responsible for the oxidation of isopropanol into acetone via the possible formation of a gem-diol, which then dehydrates into acetone. The existence of two simultaneous or alternative mechanisms for the oxidation of isopropanol may explain why titania is much more photoactive than $ZrTiO_4$.

4. Conclusions

Despite good textural properties with a Brunauer–Emmett–Teller (BET) specific area similar to that of the parent oxides and a well-adapted absorbance spectrum close to those of zirconia and titania, $ZrTiO_4$ was found to be less photoactive. This lower activity may be accounted for by a poorer photoconductive response in vacuum and in oxygen. Smaller concentrations of free photoelectric charges are produced and the subsequent photodesorption or photoactivation of oxygen is more limited. This study represents an example of an attempt to prepare a new photoactive phase starting from two active oxides (titania and zirconia) containing two isoelectronic ions (Ti^{4+} and Zr^{4+}), i.e. no doping effects by valence induction. Despite these favourable factors, it has not been possible to synthesize a new phase more photoactive than or, at least, as active as titania. These results confirm those obtained in the literature which claim that titania is (and remains) the most photocatalytically active phase, especially in the form of anatase. The best photocatalytic performance of anatase can be ascribed to the optimum combination

of a good ability to adsorb reactants and a good efficiency of absorption of photons, both based on appropriate photoelectronic properties.

Acknowledgements

J.A.N. wishes to express his gratitude to the Spanish DGICYT for partial funding of this work within the framework of Projects PB90-0911 and PB93-0917. This work was partly supported by an Integrated Action between France and Spain (French contract: AI No. 92/152; Spanish contract: HF-048 (1992)).

References

[1] N. Serpone, E. Pelizzetti (Eds.), Photocatalysis, Fundamentals and Applications, Wiley, New York, 1989.
[2] M. Schiavello (Ed.), Photocatalysis and Environment: Trends and Applications, NATO-ASI Series C, Vol. 238, Kluwer Academic, London, 1987.
[3] D.F. Ollis, H. Al-Ekabi (Eds.), Photocatalytic Purification and Treatment of Water and Air, Elsevier, Amsterdam, 1993.
[4] J.-M. Herrmann, C. Guillard, P. Pichat, in: P. Ruiz, F. Thyrion, B. Delmon (Eds.), Environmental Industrial Catalysis, Catalysis Today, Vol. 17, Elsevier, Amsterdam, 1993, p. 7.
[5] J.A. Navio, F.J. Marchena, M. Macias, P.J. Sanchez-Soto, P. Pichat, J. Mater. Sci. 27 (1992) 2463.
[6] J.-M. Herrmann, J. Disdier, P. Pichat, Chem. Phys. Lett. 108 (1984) 618.
[7] P. Pichat, J.-M. Herrmann, J. Disdier, M.N. Mozzanega, H. Courbon, in: S. Kaliaguine, A. Mahay (Eds.), Catalysis on the Energy Scene, Elsevier, Amsterdam, 1984, p. 131.
[8] W. Mu, J.-M. Herrmann, P. Pichat, Catal. Lett. 3 (1989) 73.
[9] R.I. Bickley, F.S. Stone, J. Catal. 31 (1973) 389.
[10] R.I. Bickley, G. Munuera, F.S. Stone, J. Catal. 31 (1973) 398.
[11] R.B. Cundall, R. Rudham, M.S. Salim, J. Chem. Soc., Faraday Trans. I 72 (1976) 1642.
[12] R.B. Cundall, B. Hullme, R. Rudham, M.S. Salim, J. Oil Col. Chem. Assoc. (1978) 351.
[13] T. Egerton, C.J. King, J. Oil Col. Chem. Assoc. 62 (1979) 386.
[14] G. Irick, J. Appl. Polym. Sci. (1972) 2387.
[15] H. Courbon, J. Disdier, J.-M. Herrmann, P. Pichat, J.A. Navio, Catal. Lett. 20 (1993) 251.
[16] J.A. Navio, G. Colón, in: V. Cortés Corberán, S. Vic Bellon (Eds.), New Developments in Selective Oxidation II, Elsevier, Amsterdam, 1994, p. 721.
[17] J.-M. Herrmann, J. Disdier, P. Pichat, J. Chem. Soc., Faraday Trans. I 77 (1981) 2815.
[18] J.A. Navio, F.J. Marchena, M. Macias, P.J. Sanchez-Soto, in: P. Vincenzini (Ed.), Ceramics Today Tomorrow's Ceramics, Mater. Sci. Monographs, Vol. 66B, Elsevier, Amsterdam, 1991, p. 889.
[19] J.A. Navio, M. Macias, M. Gonzalez-Catalán, A. Justo, J. Mater. Sci. 27 (1992) 3036.
[20] P. Pichat, E. Borgarello, J. Disdier, J.-M. Herrmann, N. Serpone, E. Pelizzetti, J. Chem. Soc., Faraday Trans. I 84 (1988) 261.
[21] J.-M. Herrmann, J. Disdier, M.N. Mozzanega, H. Courbon, P. Pichat, in: G. Centi, F. Trifirò (Eds.), New Developments in Selective Oxidation, Elsevier, Amsterdam, 1990, p. 675.
[22] H. Courbon, M. Formenti, P. Pichat, J. Phys. Chem. 81 (1977) 550.
[23] H. Courbon, P. Pichat, C.R. Acad. Sci. (Paris) C285 (1977) 171.
[24] J.-M. Herrmann, J. Disdier, M.N. Mozzanega, P. Pichat, J. Catal. 60 (1979) 369.
[25] G. Paraskevoupolos, R.J. Cvetanovic, J. Chem. Phys. 50 (1969) 590.